

APPLYING THE SCIENTIFIC METHOD TO ACOUSTIC REFLECTOR DESIGN

J O'Keefe O'Keefe Acoustics, Toronto Canada

1 INTRODUCTION

The performance of acoustic reflectors is well documented in the literature of acoustic science. The methods used in designing these reflectors for auditoria, however, remain mostly exercises in trial and error. Other disciplines, e.g. structural engineering, internet routing, portfolio management, etc., now employ the mathematics of Multi-objective Optimisation (MOO) and, in particular, Pareto Optimisation. These methods, along with a new 3-Dimensional curvature attenuation prediction method will be employed to study and optimise the performance of a segmented dome.

2 3-D CURVATURE ATTENUATION

A 3-Dimensional extension to Rindel's 2-D curvature attenuation calculation procedure^{1,2} has been proposed by the author in ref.[3] and will be summarised here, making reference to Figure 1. Rindel's curvature attenuation method is simple and elegant. It is based on a logarithmic comparison of the spherical divergence (or spreading) from two sources. The first spreading assumes that the reflector is flat and the virtual image source is located using the Method of Images, as it would be with any other flat reflector. The second spreading assumes that the reflector is curved and that the virtual source is located somewhere on either side of the reflector, depending on whether it is convex or concave.

2.1 Source Location

In Rindel's 2-D method, the distance between the reflection point and the "curved" image source is calculated algebraically. The exact position of the point is never obtained geometrically. There are standard methods to locate the source for curved mirrors but these only work when the source is in front of the mirror. Acoustic sources, of course, are not generally in front of a reflector. The proposed procedure for locating an oblique incidence source is described as follows:

- i) As shown in Figure 1, pick two equally spaced points, P_1 and P_2 , on either side of the desired reflection point, P_0 , and create tangential planes to the reflector at both of these points. Ensure that the points P_0 , P_1 , P_2 and S_0 are co-planar.
- ii) With the two tangential planes, create virtual image sources using the Method of Images. These are shown in Figure 1 as points S'_1 and S'_2 .
- iii) Create two infinite lines, $\overleftrightarrow{S'_1P_1}$ and $\overleftrightarrow{S'_2P_2}$.
- iv) Find the intersection of these two lines. This will be the approximate image location, S_{image} . The closer the adjacent reflection points (P_1 and P_2) are to the original reflection point P_0 , the more accurate the image location will be.

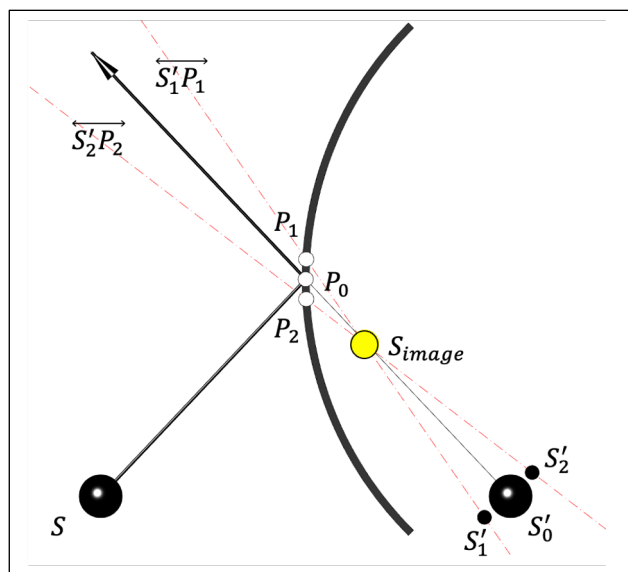


Figure 1. Image source location for a curved reflector.

It is very important that the two adjacent points, (P_1 and P_2), the source point (S_0) and the reflection point (P_0) are all on the same plane. If not, the lines generated from these points, ($\overrightarrow{S'_1P_1}$ and $\overrightarrow{S'_2P_2}$) may not intersect. Referring to Figure 2, this is best done by creating a Reflection Path Plane using the three points on the reflection path, i.e. the source, reflection and receiver points. Alternatively, if the receiver point is not available it can be replaced with the virtual source point associated with the reflection point, i.e. point S'_0 . The intersection of this plane with the reflector surface will generate a curve, C . All the points on this curve will be co-planar. To locate two co-planar points equidistant from the reflection point P_0 , find the parameter value, t , on the curve C that represents the point closest to P_0 . The two adjacent co-planar points will be located on the curve at parameter values $t + \delta t$ and $t - \delta t$, expressed as follows:

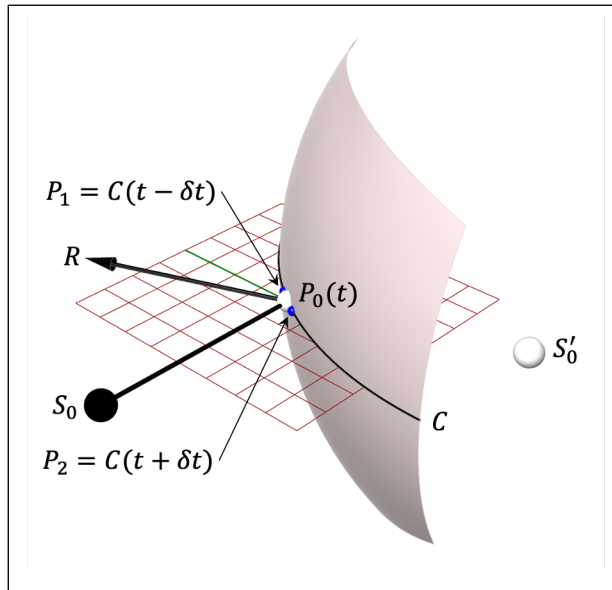


Figure 2. The Reflection Path Plane intersects the reflector to create the curve C which, in turn, is used to create the adjacent points P_1 and P_2 .

$$\begin{aligned} P_1 &= C(t + \delta) \\ P_2 &= C(t - \delta) \end{aligned} \quad (1)$$

For a curve C of unit length, the small increment δt is usually in the range of 0.05.

2.2 Comparative Divergence

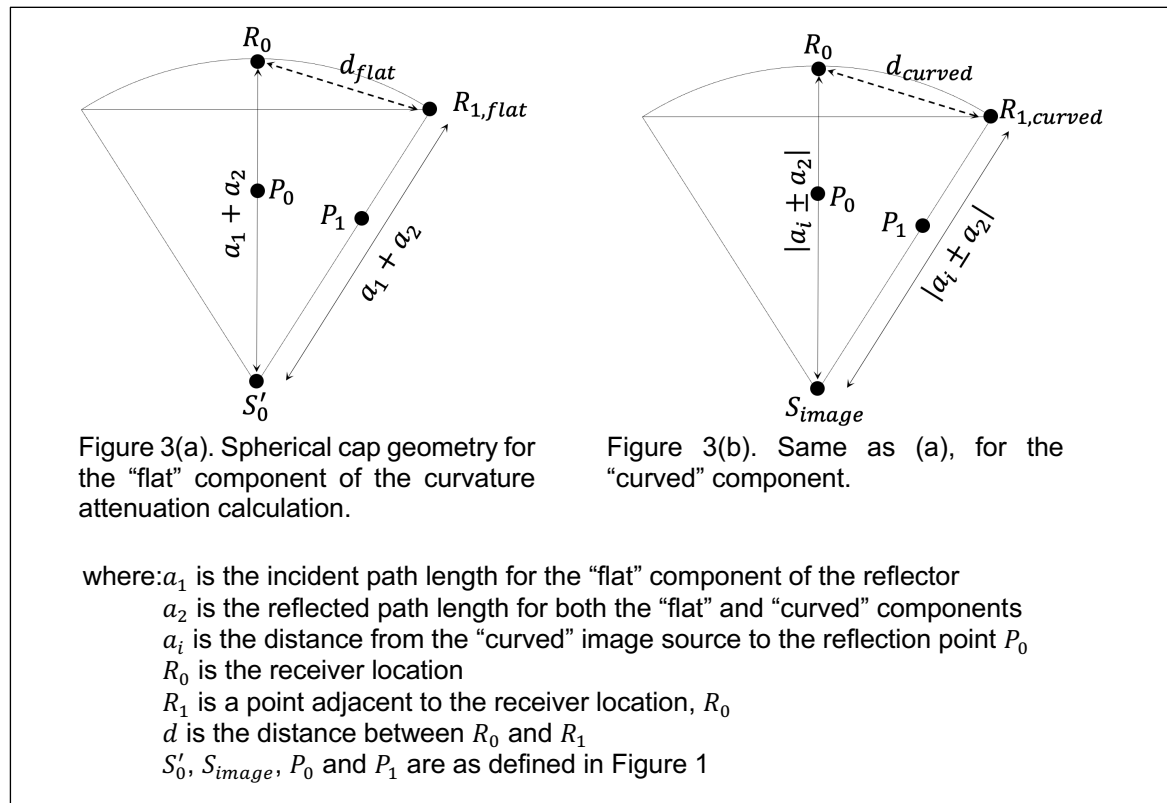
Once the sources for the “flat” and “curved” components of the reflector calculation have been determined, two cones of reflected energy are radiated out towards and terminate at the receiver location. The area of the domes or “spherical caps” at the base of these cones (i.e. at the receiver point) quantify the relative energy levels spread out from the “flat” and “curve” virtual sources. The logarithmic ratio of these two areas quantifies the curvature attenuation of the reflector. This is explained further in ref.[3].

The width of these cones is determined at their interface with the reflector. Specifically, the radius of the cone at the interface will be the distance between the reflection point P_0 and either one of the adjacent points: P_1 or P_2 .

The area of a spherical cap is:

$$A_{cap} = \pi d^2 \quad (2)$$

Where d is the distance between the peak of the cap and the edge of the cap. These are shown in Figure 3 as the points R_0 and R_1 , respectively. The point R_0 is simply the receiver point. The point R_1 is a point adjacent to the receiver point that has been generated by an adjacent point on the reflector. (In Figure 1, this would be either point P_1 or P_2 .) For example, to generate the adjacent receiver point R_1 – and referring again to Figure 1 – create a unit vector between the virtual source point S'_1 and the adjacent point P_1 . Multiply the unit vector by the distance between point S'_1 and the actual receiver, R_0 . Then, finally, use this vector to translate a copy of the virtual source point S'_1 to a location beside the actual receiver point and refer to it as the adjacent receiver point R_1 .



Using Rindel's concept of comparative divergences, the attenuation (or amplification) due to curvature will be:

$$L_{curve} = -10 \log \left(\frac{A_{curved}}{A_{flat}} \right) \quad (3)$$

where: A_{curved} is the area of the spherical cap associated with the "curved" component
 A_{flat} is the area of the spherical cap associated with the "flat" component

Combining this with equation (2) gives the proposed expression for 3-Dimensional curvature attenuation as:

$$L_{curve} = -20 \log \left(\frac{d_{curved}}{d_{flat}} \right) \quad (4)$$

3 SEGMENTED DOMES

Domes, or partial domes, are rarely found in modern performing arts venues. This is because the acousticians involved in the design of these rooms maintain a legitimate concern about the focusing problems associated with concave surfaces. There are, however, many examples of acoustically successful rooms with partial domes. Or, to use the more geometrically precise term, "spherical segments". These rooms come from a time that pre-dates the age of acousticians. Despite this, they can often offer wonderful acoustic experiences. And, with that, perhaps some acoustical lessons to be learnt.

3.1 Analysis

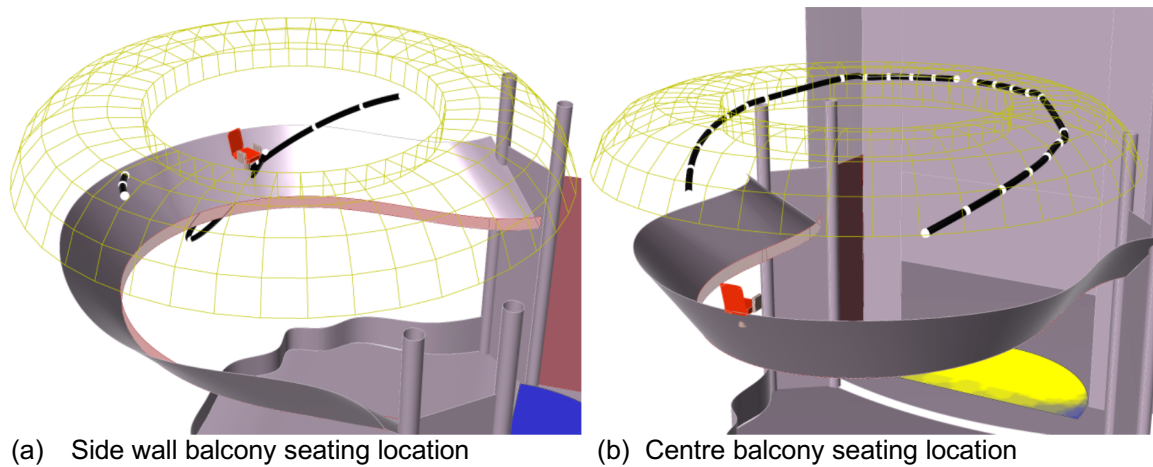


Figure 4. Focal point contour study for the upper balcony of the Théâtre Champs Elysée, Paris

The 3-D extension of Rindel's method can be used in this effort. An example is taken from the Théâtre Champs Elysée in Paris. A 3-D computer model of the room has been constructed and, in it, the segmented spherical ceiling has been populated with 500 reflection points. The curved image source location method described in Section 2.1 was used to identify any focal points that might be associated with these reflection points. The focal points are then joined together to create what might be called "focal point contours". Two examples taken from the upper balcony are shown in Figures 4 (a) and (b). In the former, note how close the focal point contour is to the listeners, passing right in front of a seating location on the house left side of the balcony. In seats closer to the centre of the balcony, where the sound is noticeably better, the focal point contours are distant from the listeners and form something like a "halo" around a listener location at the exact centre of the balcony.

3.2 Optimisation

Multi-objective optimisation methods, such as the ones used by the author in previous studies^{4,5,6,7}, can be used to encourage focal point scenarios like the one seen in Figure 4(b) and, hopefully, discourage the type of contours seen in Figure 4(a). Before doing that, however, flexible segmented domes must be built inside a computer model. This is done with the Segmented Sphere BBrep Constructor and is described as follows.

The flexible segmented sphere reflector is created from two circles and a curve, all three of which are concentric about the same axis. For example, in the case of a segmented sphere located in a ceiling, it would be a Z-Axis in the centre of that ceiling. The two circles form the upper and lower bounds of the segmented sphere. The curve is located in between the two circles and defines the middle profile of the reflector. The reflector geometry itself is constructed as follows:

- (i) the user defines a Spinal Curve and an initial U-V Axis pair. An example is shown in Figure 5(a). The U-V Axis pair is shown at the centre point of the Spinal Curve.
- (ii) the radius of this curve is modified (either randomly or through Genetic Algorithm recombination) inside a range set by the user. The initiating U-V Axis pair is then translated to a position on the newly modified Spinal Curve. (Although, in the interest of clarity, the radius will not be modified in the explanation shown in Figure 5.)
- (iii) Spinal Planes are created perpendicular to the Spinal Curve, as shown in Figure 5(b),
- (iv) The initiating U-V Axes are copied and translated onto each of the Spinal Planes. Figure 5(c)
- (v) On each of these translated U-V Axes, the end points of the two lines making up the axes are used to create a diagonal line across the given Spinal Plane. This diagonal line, in turn, is used to create three points, referred to in Figure 5(d) as p_{upper} , p_{mid} and p_{lower} .

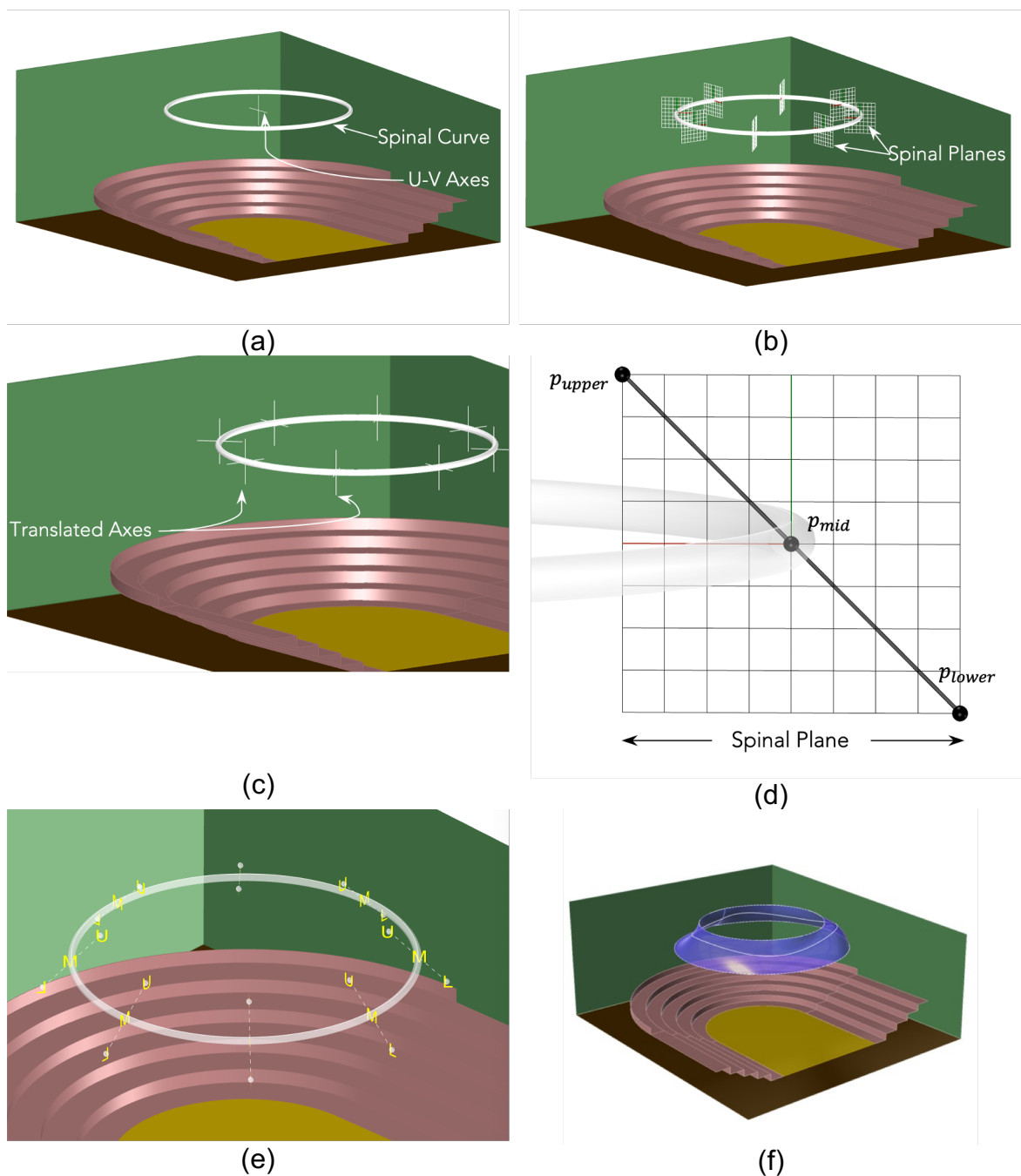


Figure 5. Construction of a reflector using the Segmented Sphere BBrep Constructor.

- (vi) Around the circumference of the segmented sphere, there will now be three points on each Spinal Plane. These are collected sequentially into the lists referred to as P_{upper} , P_{mid} and P_{lower} . The points in the lists P_{upper} and P_{lower} are used to create (circle-like) interpolated curves that will form the upper and lower Construction Curves for the reflector. The points and their interpolated curves are shown in Figure 5(e). The points are labelled "U", "M" and "L" for the lists P_{upper} , P_{mid} and P_{lower} , respectively.
- (vii) The points in the list P_{mid} are used to create the Control Point Genes⁸ that will be perturbed on their respective Spinal Planes, using their respective U and V Axes. The Control Point property (originally created as the point p_{mid} in Step v) is perturbed in each generation of the Genetic Algorithm's optimisation. These perturbed points are then collected sequentially around the circumference of the segmented sphere to create the middle Construction Curve. All three of the Construction Curves are now shown in Figure 5(f).
- (viii) The reflector surface is created using the RhinoCommon method *CreateFromLoft()*⁹, with the three Constructor Curves as its input. This final result is also shown in Figure 5(f).

The image in Figure 5(f) comes from a trial run of a so-called "Many-Objective" optimisation¹⁰. The prefix "Many" implying that there are more objectives than the three spatial dimensions that are easily conceptualized. In this case the reflector design was guided by the following five fitness functions: Single Lateral Reflection (sLF)⁴, Single Reflection Lochner Burger Ratio (sLB)⁷, Strength (sG)⁵, Area Fitness⁶ and Spreading Fitness⁵. The first three are related to the acoustical percepts of Spatial Impression, Speech Intelligibility and Acoustic Strength. The latter two are associated with the Zone to Zone optimisation procedure proposed by the author in ref. [6]. Which is to say that the reflector has not been optimised for a single point source but, rather, for a zone of acoustic sources.

The reflector in Figure 5(f) has the outward appearance of a typical segmented dome that one might find in a theatre or concert hall. On closer inspection, however, it appears to be concave in some parts and convex in others. This is demonstrated more clearly with the sectional profiles shown in Figure 6. The top row shows a cross-sectional view of the reflector looking towards the stage at the front of the room. The longitudinal section (taken at the middle of the reflector looking from the side) is seen in the third row. The sections shown in the second and fourth rows of the image are taken at the quadrants between the cross and longitudinal sections. To follow the curvature of the segmented sphere around the circumference (in a counter-clockwise direction), start with the top left hand frame of Figure 6 and move down the column to the bottom. Then return to the top right hand frame of the figure and read down to the bottom of that column.

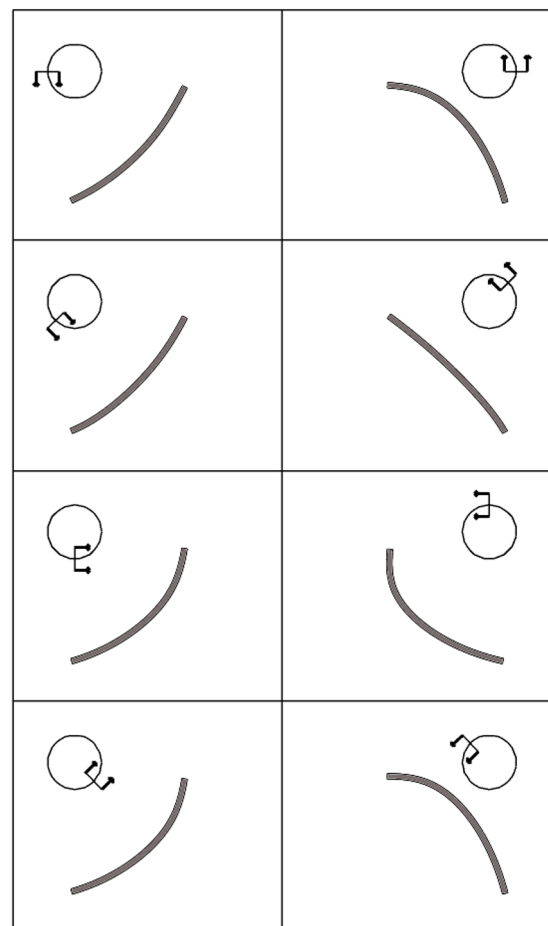


Figure 6. Sectional profiles of the optimised segmented sphere reflector shown in Figure 5(f).

4 DEMONSTRATION

To demonstrate some of the ideas discussed in this paper, the author has chosen a theatre project he is currently working on. Although, at the time of this writing, the building has yet to be named and the architectural concept of a central segmented dome may never actually be implemented. The study serves as a good demonstration vehicle, nonetheless.

In this case, a 4-objective optimisation was implemented using the Zone to Zone procedure described in ref. [6]. The first two of the 4 objectives are related to the Zone to Zone concept. The Visible Area Fitness quantifies how much of the source zone is visible to a listener, through the reflector, if he or she were looking at it like an optical mirror. The Spreading Fitness quantifies how evenly distributed the view is of the source zone, i.e. is it uniformly distributed or concentrated in a corner. The second two objectives are related to acoustic parameters. The Single Reflection Lateral Fraction (sLF) Fitness is intended to encourage laterally reflected sound and, hence, good spatial impression. The Single Reflection Lochner Burger Fitness (sLB) is intended to encourage good speech intelligibility. Which requires some explanation.

The Lochner Burger Fitness Function is based on a speech intelligibility parameter that has inexplicably fallen into disuse. In 1961, J.P.A. Lochner and J.F. Burger presented a family of curves describing how reflected energy is integrated with the direct sound to improve speech intelligibility¹¹. They developed the so-called Lochner Burger Ratio (LBR), considered by some to be a more refined version of 50 ms Distinctness coefficient (D50), originally proposed by Thiele in 1953¹². Where the D50 ratio integrates energy according to a step function – on either side of 50 ms a reflection is either good or bad with nothing in between – the LBR integrates the reflected energy gradually with curves based on the actual measured psycho-acoustic behaviour. Analog measurement technology at the time, however, could not easily accommodate Lochner and Burger's integration curves so the LBR quantifier never gained the popularity of the much simpler D50 ratio. The family of curves that they developed, however, are still useful and are employed here to encourage good speech intelligibility.

Partial results from the demonstration exercise are shown in Figure 7. The middle column illustrates some of the properties of the flat reference reflector. The right column shows the same for the optimised reflector. The first row shows the sectional profiles of the two reflectors, similar to the image in Figure 6.

In the second row, the direction of the green arrows indicates where the reflections are coming from and their lengths indicate the magnitude of the Lochner Burger values. The optimised reflector has generated a much better distribution of the reflected sound although, on average, the magnitude of the Lochner Burger values have not changed very much. The same can be said for the Single Reflection Lateral Fraction (sLF) values, although they are not shown here.

The bottom row of Figure 7 will also require some explanation. In this incarnation of the theatre, it is in its thrust stage format. Thus the stage takes the form of a rectangle at one end and a semi-circle at the other. The entirety of this stage is taken as the acoustic source zone. The Area and Spreading fitness functions in this optimisation are trying to create the best possible view of this zone as seen by the listener looking at the reflector. There are 10 listener locations in the audience area. Superimposed on each of these is a miniature outline of the source zone area. The dark patch inside each one of these outlines indicates how much of the source zone the listener can see through the reflector "mirror". There is a significant improvement in all 10 listener locations, suggesting that both the Area and Spreading Fitnesses have, indeed, encouraged a much better reflector design.

5 ACKNOWLEDGEMENTS

The author would like to thank Jean-Dominique Polack, who encouraged this work, has guided me through the doctoral dissertation associated with it and has been a wise and generous sounding board as the ideas developed.

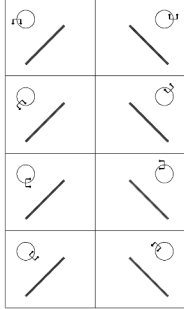
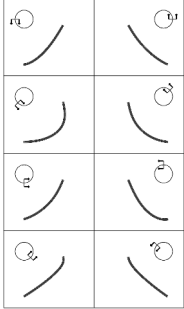
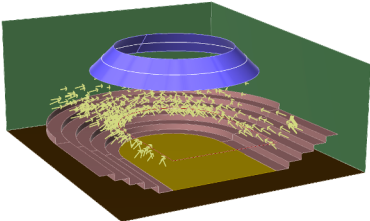
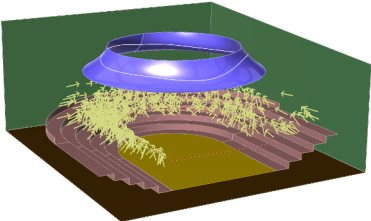
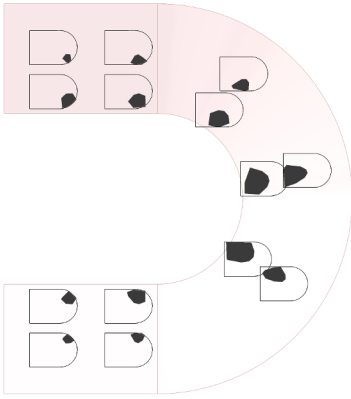
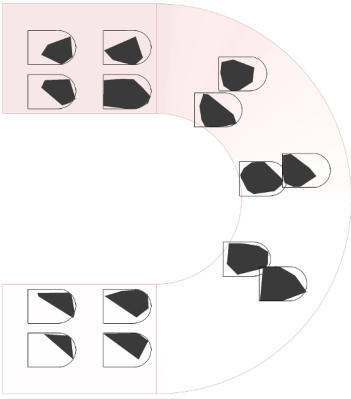
Parameter	Reference	Optimised
Reflector profiles		
Single reflection Lochner Burger values and reflection incidence directions		
Visibility of the Source Zone through the reflector		

Figure 7. Optimisation of a segmented spherical reflector.

6 REFERENCES

1. J. H. Rindel, ‘Acoustic Design of Reflectors in Auditoria’, Proc. Inst. of Acoustics, Birmingham, UK (1993).
2. J. H. Rindel, ‘Attenuation of Sound Reflections due to Diffraction’, Proc. NAM Conference, Aalborg, Denmark (1986).
3. J. O’Keefe, ‘Dômes segmentés dans les auditoriums : analyse et optimisation’, Proc. CFA Conference, Paris, France (April 2025)
4. J. O’Keefe, ‘Geometric Algorithms for Machine Based Optimisation of Acoustic Reflectors’, Proc. of International Conference on Immersive and 3D Audio (2021)
5. J. O’Keefe, ‘Genetic Algorithm Fitness Functions for acoustic reflectors in performing arts venues’, Proc. International Congress on Acoustics, Gyeongju, Korea (Oct. 2022)
6. J. O’Keefe, ‘Zone to zone reflector optimisation using a genetic algorithm’, Proc. of Institute of Acoustics; Athens (Sept. 2023)
7. J. O’Keefe, ‘Applications of a Zone to Zone Reflector Optimisation Routine’, Proc. Baltic-Nordic Acoustics Meeting, Espoo, Finland (May 2024).

8. J. O'Keefe, Doctoral dissertation, to be published.
9. Robert McNeel & Associates, "RhinoCommon API," [Online]. Available: <https://developer.rhino3d.com/api/rhinocommon/rhino.geometry.brep/createfromloft>. [Accessed 8 March 2025]
10. K. Deb and H. Jain, 'An Evolutionary Many-Objective Optimization Algorithm Using Reference-Point-Based Nondominated Sorting Approach, Part I: Solving Problems With Box Constraints', IEEE Transactions on Evolutionary Computation, vol. 18, no. 4, pp. 577-601, 2014. (NSGA-III)
11. J. Lochner and J. P. Burger, 'The Intelligibility of Speech Under Reverberant Conditions', Acustica, vol. 11, pp. 195-200, 1961
12. R. Thiele, 'Richtungsverteilung und Zeitfolge der Scallruckwürfe in Raumen (Directional Distribution and Time Sequence of Reflections in Rooms)', Acustica, vol. 3, pp. 291-297, 1953.